

A method for sea clutter elimination in the detector of high frequency surface wave radar

Ha Huy Dung^{1*}, Le Duy Hieu¹, Bui Ngoc My², Cao Viet Linh¹

¹Radar Institute/Academy of Military Science and Technology;

²Department of Education and Training/Academy of Military Science and Technology.

*Corresponding author: dungsystemdesigner@gmail.com.

Received 11 January 2022; Revised 21 January 2022; Accepted 14 February 2022.

DOI: <https://doi.org/10.54939/1859-1043.j.mst.77.2022.22-29>

ABSTRACT

In high frequency surface wave radars, the detection capability is limited by the first-order sea clutter spikes. The energy, location, and Doppler frequency of first-order sea clutter depend on the sea states, which is difficult to model using a fixed expression to eliminate sea clutter. Based on the characteristics of first-order sea clutter, the paper proposed a two-stage detector to eliminate sea clutter. The approach shows the capability to eliminate uncertain first-order sea clutter and detect targets in the vicinities of sea clutter in the Range – Doppler map.

Keywords: High frequency; Surface wave radar; Sea clutter; Adaptive CFAR.

1. INTRODUCTION

First-order sea clutter, which has high energy spikes [1, 2] often masks other targets in the close vicinities. As such the detection techniques based on the traditional Constant False Alarm Rate (CFAR) principle [3] has low detection performance in High Frequency Surface Wave Radar (HFSWR). As such, recently studies on HFSWR tend to focus on adaptive CFAR. The main research directions and their limits include:

+ Presegmentation-based adaptive CFAR [4]: This method changes the reference window's size to suppress clutter. This solution is limited by the inability to determine the clutter regions to perform an adaptive reference window. Also, the window size values do not guarantee the optimality when the clutter characteristics cannot be described mathematically;

+ Adaptive CFAR method according to environmental aspects [5, 6]: Each CFAR technique has certain advantages for different operating environment properties. Therefore, applying a specific CFAR technique to one particular environment will improve the quality of the detector. However, it's difficult to determine the environment properties to use the correct CFAR method for the sensor in practice.

+ Adaptive power regression thresholding [7]: This method reduces the energy fluctuations of clutter spikes relative to targets nearby, thus reducing the impact of the high-energy clutter domain on the average noise level. This is a support solution for CFAR techniques, but it is not an adaptive CFAR.

+ Adaptive solution using prior knowledge of sea clutter-dominated regions [4, 8]: Studies using available features of clutter spikes are two-stage detectors. These solutions focus on the elimination of heterogeneity caused by sea clutter in HFSWR. The energy equivalent method [8] did not use the characteristics of first-order sea clutter. In [4], the sea clutter is fixed, given by (1), and did not account for the sea current.

Therefore, the optimization and suitability of CFAR solutions applied to HFSWR is still an open problem. According to [9, 10], first-order sea clutter in HF band is caused by the interaction between radio waves emitted and sea waves, which is half the operating wavelength of the radars, λ_0 . It consists of two peaks with high energy corresponding to the direction of movement towards or away from the radar. The frequency of first-order sea clutter is expressed in (1) [11],

however, outside of these frequencies, sea clutter has some uncertainties caused by the sea current and is calculated by (2) [2, 12].

The paper proposed a two-stage adaptive CFAR (TSA-CFAR). The difference between the proposed methods is that the detection and elimination of first-order sea clutter are done in the presence of sea current. As such, the Doppler frequencies of first-order sea clutter will be calculated using (2) which is not fixed. In Section 2, we will present the principle of the detector in the first stage using the 3 detectors in parallel to detect all targets and first-order sea clutter. In the second stage we will use first-order sea clutter's characteristics to detect and eliminate it. Section 3 is the implementation results based on simulations. The remarks and future research will be presented in Section 4.

2. A TWO STAGE DETECTOR

The Doppler frequency, f_{Br1} , of first-order sea clutter is calculated as [11]:

$$f_{Br1} = \pm \sqrt{\frac{g}{\pi\lambda_0}} \quad (1)$$

In the presence of sea current, the Doppler frequency is expressed as follows [2, 12]:

$$f_{Br1} = \pm \sqrt{\frac{g}{\pi\lambda_0}} - \frac{2V_c}{\lambda_0} \cos \alpha \quad (2)$$

where: $g = 9.81 \text{ m/s}^2$ is the gravitational acceleration, V_c is the current speed, and α is the angle between the current direction and the grazing angle of the radar.

We will detect and eliminate the sea clutter, which has the frequencies described in (2). The detection process will be done will Range-Doppler data (RD map) [13]. The proposed TSA-CFAR detector consists of 2 stages, and its general structure is illustrated in figure 1:

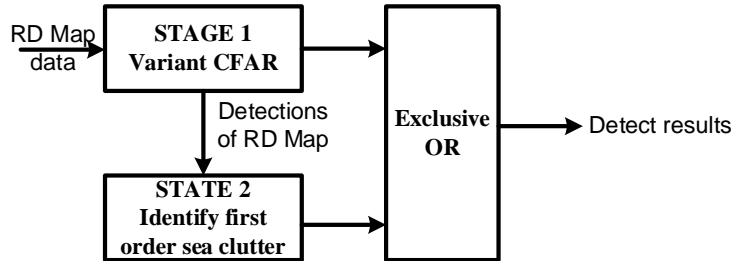


Figure 1. TSA-CFAR detector's general structure.

+ Stage 1: We use three sets of OS-CFAR in parallel, including one original OS-CFAR with Cell Under Test (CUT) in the middle of the reference window [14], two OS-CFARs with CUT located at the left and right borders of the reference window, respectively. Target detection results are determined when any of the three OS-CFARs confirms the target's existence in CUT. The OS-CFAR technique was chosen because of its good performance in the case of many closely positioned targets, and its parameter set is highly customizable during operation. According to [14], the calculation for P_{fa} as a function of detector parameters is described as:

$$P_{FA} = k \binom{N}{k} \frac{(k-1)!(T_{OS} + N - k)!}{(T_{OS} + N)!} \quad (3)$$

where: T_{OS} is the fixed detection threshold; N is the reference window size; k is the noise assessment position after the reference cells have been ranked based on their energy level. It can

be seen that with a selected P_{fa} , there will be many usable sets of N , k , T_{os} values as illustrated in figure 2. This approach uses three sets of OS-CFAR simultaneously to detect all targets, especially those located in the energy spike areas or two targets located too close to each other.

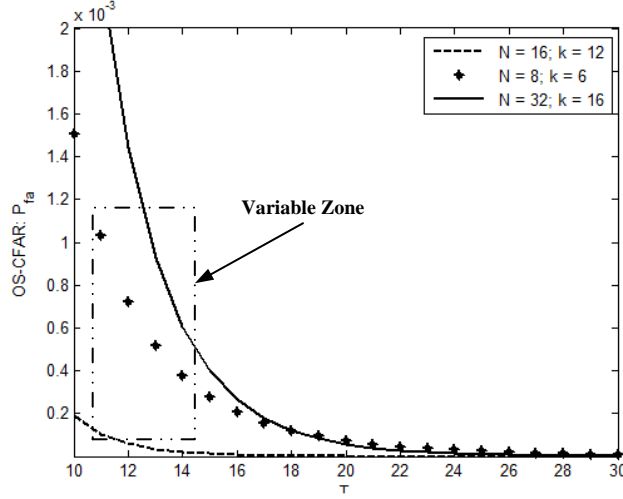


Figure 2. The relations between the parameters in OS-CFAR.

In a homogenous environment, it's easy to detect a target using the set of 3 OS-CFARs. When a target is masked because its energy is below the detection threshold in one OS-CFAR detector, it will be detected in the other CFAR, which ranks the cells in the opposite direction. The combination of detection results also ensures the detection of clutter formation in the range profile. A sensor using a combination of 3 OS-CFARs, as illustrated in figure 3, will not miss any targets, and we only use one type of CFAR detector. Also, all sea clutter information will be detected as well after the first stage of the TSA-CFAR.

The second stage of TSA-CFAR uses the following criteria to detect first-order sea clutter [10]:

- + First criterion: The first-order sea clutter that appears will spread in a large range area;
- + Second criterion: The first-order sea clutter has a two-line spectral form:
 - The negative Doppler frequency domains with its spectrum (D_x) and its spectrum spreading (Δx): $D_x + \Delta x$;
 - The positive Doppler frequency domains with its spectrum (D_y) and its spectrum spreading (Δy): $D_y + \Delta y$;

The first-order clutter filtering steps are performed as follows:

+ Step 1: Determine the Doppler frequency, which can possibly be first-order sea clutter: From the range-doppler map data in the matrix form of $N_R \times N_D$ with N_R , N_D is the number of range cells and Doppler cells, respectively. Each Doppler frequency in the RD map is a vector with N_R range cells. The vectors corresponding to $D_x + \Delta x$ and $D_y + \Delta y$ will be checked in the range dimension for the presence of possible clutter. D_x is the negative Dopplers. The central frequencies D_x , D_y are calculated using (1), (2) and rewritten as (4):

$$\begin{cases} D_x = -\sqrt{\frac{g}{\pi\lambda_0}} - A \frac{2V_c}{\lambda_0} \cos \alpha \\ D_y = \sqrt{\frac{g}{\pi\lambda_0}} - A \frac{2V_c}{\lambda_0} \cos \alpha \end{cases} \quad (4)$$

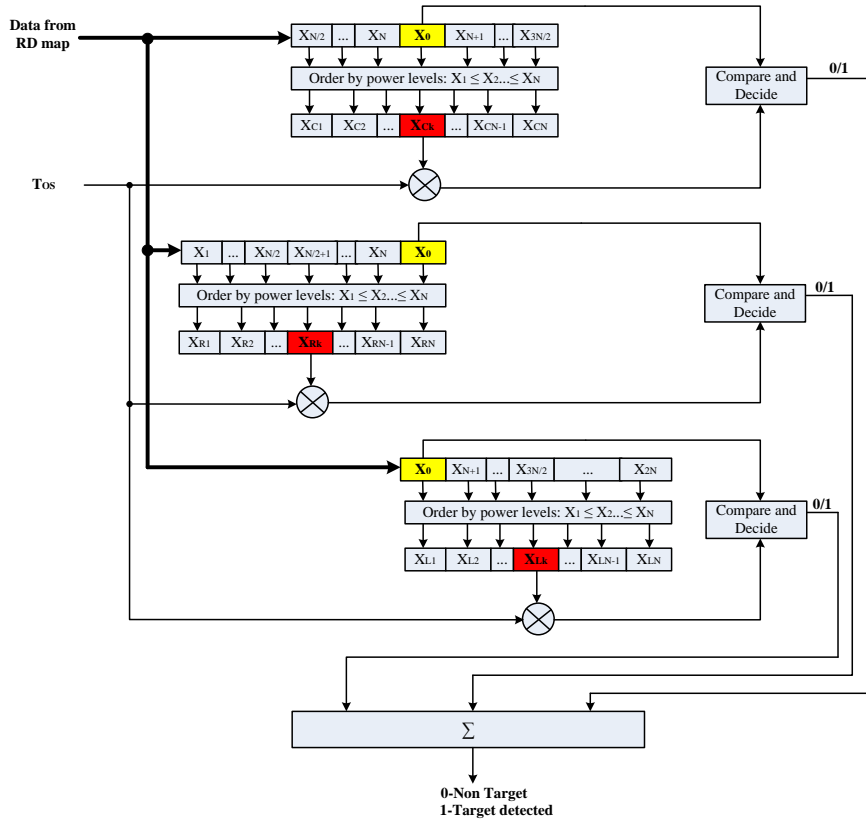


Figure 3. The first stage of a TSA-CFAR detector.

A will be zero when there is no sea current, and it will be 1 when sea current presents.

Subtract two equations to eliminate the uncertainty of the sea current, obtained D_y as in (5) corresponds to each value D_x is checked.

$$D_y = 2\sqrt{\frac{g}{\pi\lambda_0}} + D_x \quad (5)$$

The criteria for determining the frequency pair as the spectrum of first-order sea clutter is the number of range cells that exist in target detection at $D_x + \Delta x$ and $D_y + \Delta y$ must both exceed a pre-selected threshold.

+ Step 2: The frequencies in the RD map are likely to be the spectrum of first-order sea clutter will be further evaluated using the following condition: the number of consecutive detected range cells in the suspected frequency exceeds a pre-selected threshold. Any detections that meet this condition will be eliminated.

The final result left only the target markers, and all first-order sea clutter regions are eliminated. The implementation of the TSA-CFAR using Matlab simulated data is presented and evaluated in the next section.

3. PERFORMANCE ASSESSMENT OF TSA-CFAR IN HFSWR

To evaluate the detector's performance, we generate a simulation database for an HFSWR system consisting of 32 uniform linear array antenna elements with a carrier frequency of 3.5 MHz. We generated ten targets in the presence of first-order sea clutter. The targets are positioned close to each other and close the clutter regions. The first-order sea clutter is

generated with the following parameters: In the range between 0÷50 km, there is no sea current. The wind direction is 60^0 relative to the beam direction. In the range between 50÷80 km, there is no sea current. The wind direction is 0^0 relative to the beam direction. In the range between 80÷250 km, the sea current presents with a wind velocity of 2 m/s. The wind direction is of 60^0 relatives to the beam direction.

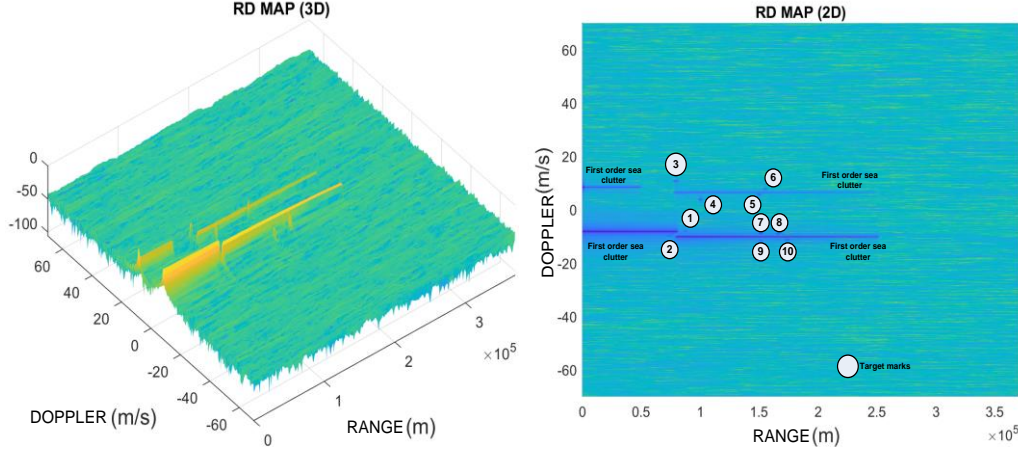


Figure 4. Simulated RD Map in HFSWR.

After filtering and FFT processing, the received signals are presented in the form of a Range-Doppler Map [1], illustrated in figure 4. As we can see, the sea clutter can appear randomly, not just in the symmetrical form.

In HFSWR, sea clutter energy typically amounts to 33% of the energy values sorted by OS-CFAR [15], along with the spreading spectrum characteristic of information processing through Fast Fourier Transform (FFT), the N , k , and T_{OS} set will differ from the relationship in equation (2). We investigated the $[N, k, T_{OS}]$ and selected the sets that meet the detection requirements, which are:

[12;6;4], [12;8;3], [12;8;4], [12;9;3], [16;8;4], [16;8;5], [16;8;6], [16;10;3], [16;10;4], [16;10;5], [16;12;3], [16;12;4], [16;12;5], [24;8;7], [24;8;8], [24;8;9], [24;8;10], [24;12;4], [24;12;5], [24;12;6], [24;12;7], [24;16;5], [24;16;6], [24;18;3], [24;18;4], [24;18;5], [24;18;6], [32;16;3], [32;16;4], [32; 16;5], [32;16;6], [32;16;7], [32;16;8], [32;16;9], [32;21;3], [32;21;4], [32;21;5], [32;21;6], [32;24;3], [32;24;4], [32;24;5], [32;24;6], [32;24;7].

From the results, we can see that:

+ First, all N that is smaller or equal to 8 are not suitable to use in HFSWR because of the spectrum spreading phenomenon that happens in FFT for target and clutter signals;

+ Second, the (N, k, T) relation closely follows formula (3), as expected with an OS-CFAR. However, the k, T relation is somewhat different because the CUT's position can sometimes be in the spectrum spreading of the target. If we chose T according to (3), the threshold would be higher than the target's energy level, thus detecting it.

+ Third, $k \leq 3N/4$. This is consistent with the statistical estimates of the clutter energy in HFSWR systems.

+ Fourth, the TSA-CFAR offers flexibility when choosing the parameter sets. This ensures the practical application of the proposed solution.

Next, we will present the results of the detecting process in TSA-CFAR with the parameter set: $N = 32, k = 16; T = 7$.

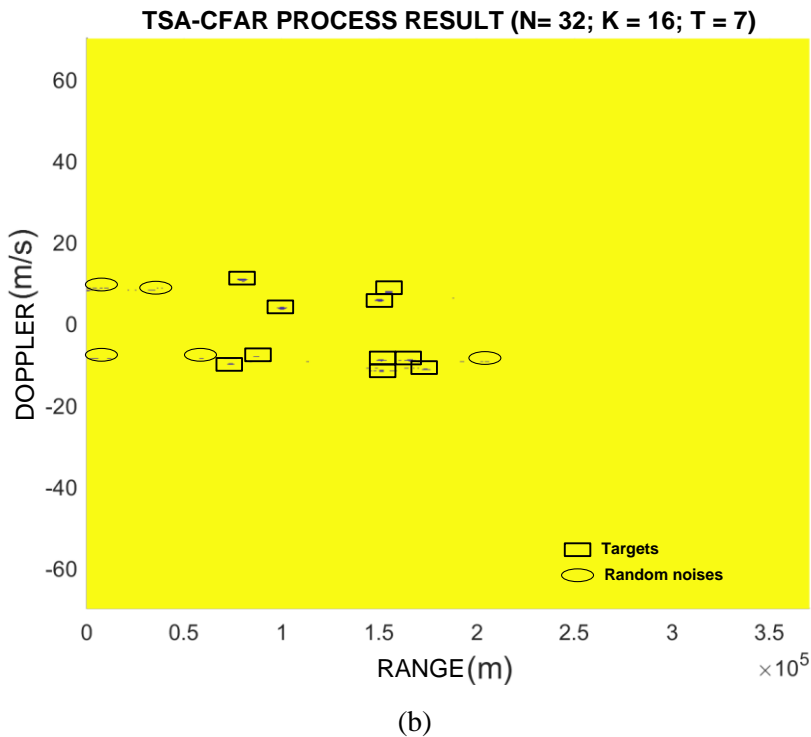
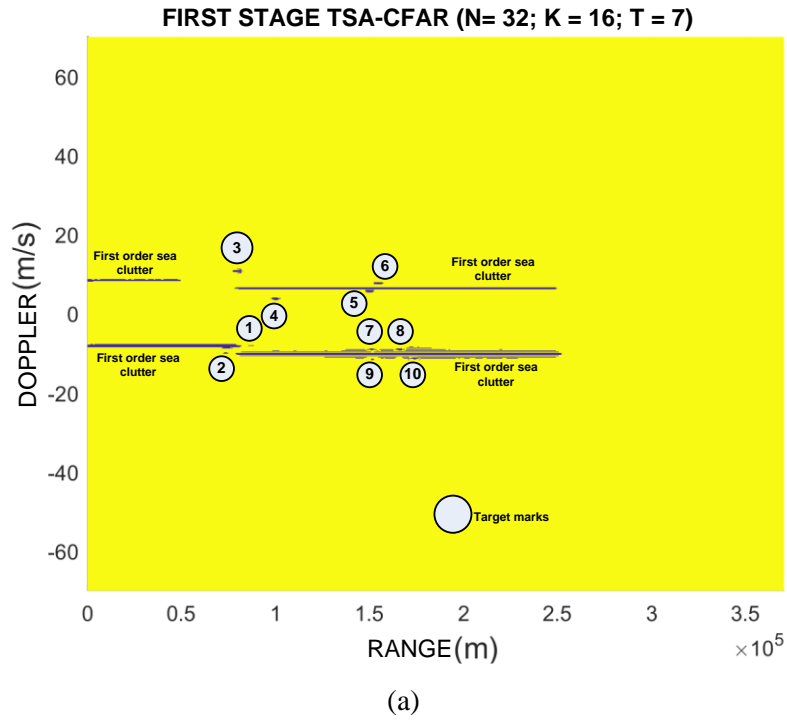


Figure 5. Detection results in TSA-CFAR for the first stage and second stage.

After the first stage of the TSA-CFAR, all targets are present in the detection map. And the first-order sea clutter region also presents showing its symmetric two-line spectral form, as illustrated in figure 5(a). Using these criteria, in the second stage, the TSA-CFAR implements the algorithm described in Section 2 to eliminate all unwanted clutter. The filter criteria as follows:

- + Spectrum spreading factor $\Delta x = \Delta y = 8$ [1];
- + Detection factor for possible first-order sea clutter TC1 = 20;
- + Threshold to eliminate clutter TC2 = 8;

The final results are presented in figure 5(b). We can see that the clutter is eliminated, leaving the real targets without missing any information. There are still some detection marks on the map. They are random noise that can be further eliminated using correlation processing.

To further demonstrate the advantage of this approach, figure 6 presents the detection results of the traditional OS-CFAR and Variability Index CFAR (VI-CFAR) [6] as a comparison. Figure 6(a) presents the detection results of a single OS-CFAR. As we can see, the traditional OS-CFAR can not detect the targets in the vicinity of the clutter edge (target No2). It also presents the clutter edges as false targets. Detections like that can be challenging to differentiate from real targets. In figure 6(b), the VI-CFAR can not eliminate all the sea clutter, and the detection of targets adjacent to the clutter region is unstable.

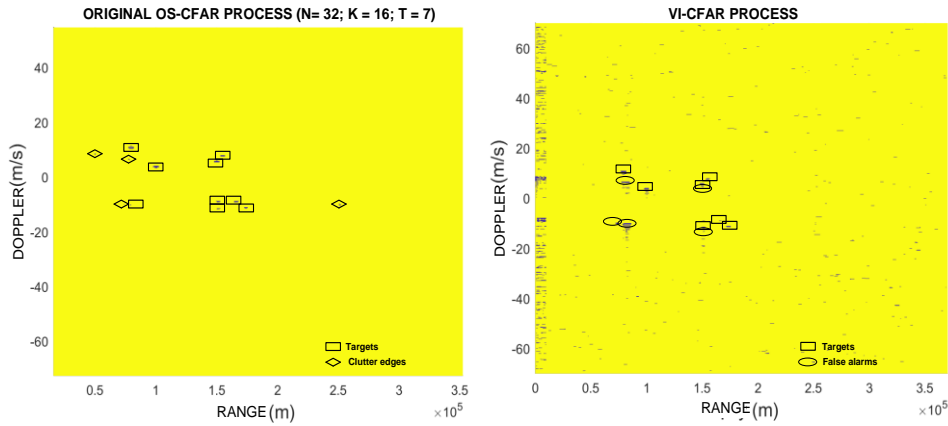


Figure 6. Detection results using traditional CFAR and VI-CFAR methods.

4. CONCLUSION

HFSWR's heterogeneous operating environment has set the requirement for the use of highly adaptive CFAR detectors. Based on the CFAR technique and the shortcomings of the previous studies, the paper proposed a solution to construct a two-stage TSA-CFAR detector. In the first stage, using the detection results of 3 OS-CFAR, all targets, including the ones close to the first-order sea clutter's edge, are detected. Also, in this stage, the proposed method can fully detect all first-order sea clutter. The information of this stage is the basis to evaluate, detect first-order sea clutter, and eliminate it in the second stage. The authors presented the structure of the detector and evaluated its performance using simulation data by comparing it with other approaches. The simulations showed that the TSA-CFAR solution could detect the targets in the clutter vicinity and eliminate all false detections caused by first-order sea clutter.

The future work includes surveying and evaluating the detection ability and studying the method of parameter correction for a two-stage detector to have a small effective reflectance area, and research on the construction of a full model of the HFSWR signal types based on actual data usage.

REFERENCES

- [1]. H.H. Dũng, L.D. Hiệu, C.V. Linh, B.N. Mỹ, "Xây dựng tín hiệu mô phỏng đặc trưng và đánh giá mô hình nhiễu biển bậc nhất trong ra đa biển tầm xa sóng bề mặt tần số cao", Tạp chí Nghiên cứu KH&CN quân sự, Số 73,06-2021 (in Vietnamese).

- [2]. Xie J., Ji Z. (2013), “*First order ocean surface cross-section for shipborne HFSWR*”, Electronics letters Vol.49-No.16.
- [3]. Xiaoli L., (2009), “*Enhanced Detection of Small Targets in Ocean Clutter for High Frequency Surface Wave Radar*” A Dissertation Submitted in Partial Fulfillment of the Requirements for the Degree of Doctor of Philosophy in the Department of Electrical and Computer Engineering, pp. 67-87.
- [4]. Hinz J.O., Holters M., Zolzer U., Gupta A. and Fickenscher T., (2012) “*Presegmentation-based adaptive CFAR detection for HFSWR*” IEEE Radar Conference.
- [5]. Mashade M. B. EL, (1995) “*Analysis of the censored-mean level CFAR processor in multiple target and nonuniform clutter*”, Radar, Sonar and Navigation, IEE Proceedings, Vol: 142 Issue: 5, pp. 259 -266.
- [6]. Cheeseman A. (2017), “*Adaptive Waveform Design and CFAR Processing for High Frequency Surface Wave Radar*”, Graduate Department of The Edward S. Rogers Sr. Department of Electrical & Computer Engineering University of Toronto.
- [7]. Dzvonnkovskaya A. and Rohling H., (2006) “*Target detection with adaptive power regression thresholding for HF radar*”, International Conference on Radar.
- [8]. A. Gupta, (2015), *Theory and Measurement Validation of Novel HFSWR Receiver Architecture: Antenna Design, Clutter Suppression and Detection*, Department of Electrical Engineering of Helmut Schmidt University, Germany, pp. 80-100.
- [9]. L. Sevgi, A. Ponsford, A. Chan, “*An integrated maritime surveillance system based on high frequency surface wave radars, Part 1 - Theory of operation*”, IEEE Proc. Ant. And Prop., Vol. 43, Aug. 2001.
- [10]. A. Ponsford, L. Sevgi, A. Chan, “*An integrated maritime surveillance system based on high frequency surface wave radars, Part 2 - Operational status and system performance*”, IEEE Proc. Ant. And Prop., Vol. 43, Oct 2001.
- [11]. Ponsford A. M., Wang J., (2010), “*A review of high frequency surface wave radar for detection and tracking of ships*”, Turkish Journal of Electrical Engineering and Computer Sciences.
- [12]. Wang Y., Mao X., Zhang J., Ji Y., (2018) “*Detection of Vessel Targets in Sea Clutter Using In Situ Sea State Measurements With HFSWR*”, IEEE Geoscience and Remote Sensing Letters.
- [13]. N. Stojkovic, D. Nikolic, P. Petrovic, N. Tosic, I. Gluvacevic, N. Stojiljkovic, “*An Implementation of DBF and CFAR Models in OTHR Signal Processing*”, IEEE 15th International Colloquium on Signal Processing & its Applications (CSPA 2019), 8 -9 March 2019, Penang, Malaysia.
- [14]. Richards M. A., (2015) “*Fundamentals of Radar system processing*” second Edition, Mc Graw Hill Education, pp. 354-360.
- [15]. OTHR-ST-Specification, “*Part 7-Signal Processing, Detection and Tracking*”, HELZEL Messtechnik 2018.

TÓM TẮT

Phương pháp loại bỏ nhiễu biển bậc nhất trong bộ phát hiện của ra đa sóng bề mặt tần số cao

Trong ra đa sóng bề mặt tần số cao, khả năng phát hiện mục tiêu bị giới hạn bởi năng lượng vượt trội của nhiễu biển bậc nhất. Do nhiễu biển bậc nhất có năng lượng, vị trí và độ dịch tần phụ thuộc vào trạng thái biển, việc sử dụng công thức cố định tính toán để loại bỏ nhiễu này sẽ không đạt được hiệu quả. Dựa vào các đặc trưng riêng biệt của nhiễu biển bậc nhất, bài báo đề xuất một bộ phát hiện hai giai đoạn để loại bỏ nhiễu. Giải pháp được nghiên cứu cho thấy, khả năng loại bỏ nhiễu biển bậc nhất bất định và phát hiện đầy đủ được những mục tiêu nằm lân cận vị trí nhiễu trong bản đồ Cự ly-Doppler.

Từ khóa: Tần số cao; Ra đa sóng bề mặt; Nhiễu biển; CFAR thích nghi.